Optics Communications 361 (2016) 28–35

Contents lists available at ScienceDirect

Optics Communications

journal homepage: www.elsevier.com/locate/optcom

A novel method for finding the initial structure parameters of optical systems via a genetic algorithm

LIU Jun [a,b,c,*], Wei Huang [b,c], Fan Hongjie [b,c]

[a] University of Chinese Academy of Sciences, Beijing 100049, China
[b] Changchun Institute of Optics, Fine Mechanics and Physics, Chinese Academy of Sciences Changchun, Jilin 130033, China
[c] State Key Laboratory of Applied Optics, Changchun, Jilin 130033, China

ARTICLE INFO

Article history:
Received 22 April 2015
Received in revised form
5 October 2015
Accepted 11 October 2015
Available online 23 October 2015

Keywords:
Geometric optics
Aberrations (global)
Computation methods
Mirror system design

ABSTRACT

A novel method for finding the initial structure parameters of an optical system via the genetic algorithm (GA) is proposed in this research. Usually, optical designers start their designs from the commonly used structures from a patent database; however, it is time consuming to modify the patented structures to meet the specification. A high-performance design result largely depends on the choice of the starting point. Accordingly, it would be highly desirable to be able to calculate the initial structure parameters automatically. In this paper, a method that combines a genetic algorithm and aberration analysis is used to determine an appropriate initial structure of an optical system. We use a three-mirror system as an example to demonstrate the validity and reliability of this method. On-axis and off-axis telecentric three-mirror systems are obtained based on this method.

1. Introduction

The damped-least-squares (DLS) method, as the most popular optimisation algorithm, is extensively used in modern optical design software [1–3]. The DLS method used in the optimisation process involves searching for the minimum of the error function in a multi-dimensional variable space. However, the result obtained via the DLS method is usually a local minimum lying close to the starting point. In other words, the result from the use of commercial optical design software to optimise an optical system is strongly affected by the choice of the initial structure. Sometimes, the initial structure plays the most important role in our optical design process. Typically, optical designers obtain the initial structure parameters of optical systems by referring to existing structures included in overdue patents and collections, and then optimising these structures for their own applications via commercial optical design software. However, this process is time consuming, and a similar structure is not likely to be determined consistently. Accordingly, it would be highly desirable to find a practical and efficient method to calculate the initial structure parameters automatically.

In this paper, we propose an automatic method to calculate the initial structure parameters via GA. GA, introduced by Professor J. Holland in 1975 [4,5], is a powerful optimisation tool for finding the global minima in a high-dimensional, and highly nonlinear parameter space. GA has been introduced into the area of optical system design [6–12], such as optimisation for diffractive optical elements [6], optimisation for a wavefront coding system [7], and optimisation for focusing through turbid media in noisy environments [8]. Here, we use GA to search for high potential initial structures. A three-mirror system is employed as the example to implement the idea. The third-order aberration expressions of the three-mirror system with an aperture stop on the primary mirror are given by aberration analysis. The error function, which indicates the performance of the optical system, is composed of weighted aberrations and some constraints defined flexibly to meet the configuration requirement. The lower the value of the error function is, the higher the image quality of the system. GA is then used to find the suitable initial structure by minimising the error function. With this method, initial structures of three-mirror systems are calculated conveniently. After a further optimisation by commercial optical design software CODE V [13] based on the initial structure, on-axis and off-axis telecentric three-mirror systems are obtained.

This paper consists of four parts. In Section 2, we discuss the fundamental principle of our work. In Section 3, two design examples of three-mirror systems are presented: an on-axis three-mirror system with a 1000 mm focal length, 200 mm aperture and 1° field of view (FOV) and an off-axis telecentric three-mirror system with a 1000 mm focal length, 150 mm aperture and $1° \times 20°$ FOV are designed. Section 4 presents the conclusion of our work.

* Corresponding author at: Changchun Institute of Optics, Fine Mechanics and Physics, Chinese Academy of Sciences Changchun, Jilin 130033, China.
E-mail address: ciomplj@sina.com (L. Jun).

http://dx.doi.org/10.1016/j.optcom.2015.10.036
0030-4018/

2. Principle

2.1. Aberration analysis for three-mirror system

Three-mirror systems are widely used in various fields, such as biological microscopy, thermal imaging systems, infra-red multi-spectral detection, space photography, lithography, and optical remote sensing. The advantages of this system include being free of chromatic aberrations, a large aperture, a small volume, loose heat tolerance, a large rectangular FOV, etc. It is also helpful in solving the obstruction problem by making the FOV off-axis. Using the three-mirror system, it becomes easier to obtain optical systems of high image quality that are also lighter in weight.

The layout of the three-mirror system is shown in Fig.1. The system is composed of three mirrors: a primary mirror (M_1), a secondary mirror (M_2), and a tertiary mirror (M_3). The obscure ratios of M_1 and M_2 are α_1 and α_2 respectively, the magnifications of M_2 and M_3 are β_1 and β_2, respectively, and the conic coefficients employed in the structure of each mirror are $-e_1^2$, $-e_2^2$ and $-e_3^2$, where,

$$\begin{cases} \alpha_1 = \dfrac{l_2}{f_1'} \approx \dfrac{h_2}{h_1}, \quad \beta_1 = \dfrac{l_2'}{l_2} = \dfrac{u_2}{u_2'} \\ \alpha_2 = \dfrac{l_3}{l_2'} \approx \dfrac{h_3}{h_2} \quad \beta_2 = \dfrac{l_3'}{l_3} = \dfrac{u_3}{u_3'} \end{cases} \tag{1}$$

Assuming that the focal length of a three-mirror system is f', based on the definition of magnification and obstruction ratios, the expressions for the radii of curvature of different mirrors and their corresponding thicknesses are calculated according to the paraxial optical theory:

$$\begin{cases} R_1 = \dfrac{2f'}{\beta_1\beta_2} \\ R_2 = \dfrac{2\alpha_1 f'}{\beta_2(1+\beta_1)} \\ R_3 = \dfrac{2\alpha_1\alpha_2 f'}{1+\beta_2} \end{cases} \tag{2}$$

$$\begin{cases} d_1 = \dfrac{(1-\alpha_1)f'}{\beta_1\beta_2} \\ d_2 = \dfrac{\alpha_1(1-\alpha_2)f'}{\beta_2} \\ d_3 = \alpha_1\alpha_2 f' \end{cases} \tag{3}$$

The third-order aberration coefficients are given by the following expressions [14]:

$$\begin{cases} S_{\mathrm{I}} = \sum hP + \sum h^4 K \\ S_{\mathrm{II}} = \sum yP - J\sum W + \sum h^3 yK \\ S_{\mathrm{III}} = \sum \dfrac{y^2}{h}P - 2J\sum \dfrac{y}{h}W + J^2\sum \varphi + \sum h^2 y^2 K \\ S_{\mathrm{IV}} = \sum \dfrac{\Pi}{h} \\ S_{\mathrm{V}} = \sum \dfrac{y^3}{h^2}P - 3J\sum \dfrac{y^2}{h^2}W + J^2\sum \dfrac{y}{h}(3\varphi + \dfrac{\Pi}{h}) \\ \qquad -J^3\sum \dfrac{1}{h^2}\Delta\dfrac{1}{n^2} + \sum hy^3 K \end{cases} \tag{4}$$

where h is the height of the marginal ray in each mirror, and y is the height of the chief ray in each mirror; both h and y are related to the parameters α_1, α_2, β_1 and β_2. Assume that the stop of the three-mirror system is on the primary mirror.

$$\begin{cases} y_1 = 0 & h_1 = 1 \\ y_2 = \dfrac{\alpha_1 - 1}{\beta_1\beta_2} & h_2 = \alpha_1 \\ y_3 = \dfrac{\alpha_2(\alpha_1-1) + \beta_1(1-\alpha_2)}{\beta_1\beta_2} & h_3 = \alpha_1\alpha_2 \end{cases} \tag{5}$$

$$\begin{cases} P = \left(\dfrac{\Delta u}{\Delta\frac{1}{n}}\right)^2 \Delta\dfrac{u}{n} \quad W = \dfrac{\Delta u}{\Delta\frac{1}{n}}\Delta\dfrac{u}{n} \\ \Pi = \dfrac{\Delta(un)}{nn'} \qquad \varphi = \dfrac{1}{h}\Delta\dfrac{u}{n} \\ K = -\dfrac{e^2}{R^3}\Delta n \end{cases} \tag{6}$$

Substituting h, y, P, W, Π, φ and K into Eq. (4) by Eq. (5) and Eq. (6), we can obtain the third-order aberrations expressed in terms of the structure parameters α_1, α_2, β_1, β_2, $-e_1^2$, $-e_2^2$, and $-e_3^2$ by tracing the marginal and chief rays.

$$\begin{cases} S_{\mathrm{I}} = \frac{1}{4}[(e_1^2-1)\beta_1^3\beta_2^3 - e_2^2\alpha_1\beta_2^3(1+\beta_1)^3 + e_3^2\alpha_1\alpha_2(1+\beta_2)^3 \\ \qquad + \alpha_1\beta_2^3(1+\beta_1)(1-\beta_1)^2 - \alpha_1\alpha_2(1+\beta_2)(1-\beta_2)^2] \\ S_{\mathrm{II}} = -\dfrac{e_2^2(\alpha_1-1)\beta_2^3(1+\beta_1)^3}{4\beta_1\beta_2} - \dfrac{[\alpha_2(\alpha_1-1)+\beta_1(1-\alpha_2)](1+\beta_2)(1-\beta_2)^2}{4\beta_1\beta_2} \\ \qquad + e_3^2\dfrac{[\alpha_2(\alpha_1-1)+\beta_1(1-\alpha_2)](1+\beta_2)^3}{4\beta_1\beta_2} + \dfrac{(\alpha_1-1)\beta_2^3(1+\beta_1)(1-\beta_1)^2}{4\beta_1\beta_2} - \frac{1}{2} \end{cases}$$

$$\begin{cases} S_{\mathrm{III}} = -e_2^2\dfrac{\beta_2(\alpha_1-1)^2(1-\beta_1^3)}{4\alpha_1\beta_1^2} - \dfrac{[\alpha_2(\alpha_1-1)+(1-\alpha_2)\beta_1]^2(1+\beta_2)(1-\beta_2)^2}{4\alpha_1\alpha_2\beta_1^2\beta_2^2} \\ \qquad - \dfrac{[\alpha_2(\alpha_1-1)+\beta_1(1-\alpha_2)](1-\beta_2)(1+\beta_2)}{\alpha_1\alpha_2\beta_1\beta_2} + \dfrac{\beta_2(1+\beta_1)}{\alpha_1} - \dfrac{1+\beta_2}{\alpha_1\alpha_2} - \beta_1\beta_2 \\ \qquad + e_3^2\dfrac{[\alpha_2(\alpha_1-1)+\beta_1(1-\alpha_2)]^2(1+\beta_2)^3}{4\alpha_1\alpha_2\beta_1^2\beta_2^2} + \dfrac{\beta_2(\alpha_1-1)^2(1+\beta_1)(1-\beta_1)^2}{4\alpha_1\beta_1^2} \\ \qquad - \dfrac{\beta_2(\alpha_1-1)(1-\beta_1)(1+\beta_1)}{\alpha_1\beta_1} \end{cases}$$

$$\begin{cases} S_{\mathrm{IV}} = \beta_1\beta_2 - \dfrac{\beta_2(1+\beta_1)}{\alpha_1} + \dfrac{1+\beta_2}{\alpha_1\alpha_2} \\ S_{\mathrm{V}} = \dfrac{2(\alpha_1-1)(\beta_1+1)}{\alpha_1^2\beta_1} + \dfrac{1}{4}\dfrac{(\beta_1+1)(\alpha_1-1)^3(\beta_1-1)^2}{\alpha_1^2\beta_1^3} \\ \qquad + \dfrac{3(\alpha_1-1)^2(\beta_1-1)(\beta+1)}{2\alpha_1^2\beta_1^2} \\ \qquad + \dfrac{2(\beta_2+1)(\alpha_2-\beta_1-\alpha_1\alpha_2+\alpha_2\beta_1)}{\alpha_1^2\alpha_2^2\beta_1\beta_2} \\ \qquad + \dfrac{3(\beta_2-1)(\beta_2+1)(\alpha_2-\beta_1-\alpha_1\alpha_2+\alpha_2\beta_1)^2}{2\alpha_1^2\alpha_2^2\beta_1^2\beta_2^2} \\ \qquad - \dfrac{e_2^2(\alpha_1-1)^3(\beta_1+1)^3}{4\alpha_1^2\beta_1^3} \\ \qquad (\beta_2+1)[(\beta_2-1)^2 - e_3^2(\beta_2+1)^2] \\ \qquad + \dfrac{(\alpha_2-\beta_1-\alpha_1\alpha_2+\alpha_2\beta_1)^3}{4\alpha_1^2\alpha_2^2\beta_1^3\beta_2^3} \end{cases} \tag{7}$$

The error function is composed of weighted aberrations and some constraints imposed by the configuration requirement, which can be expressed as F,

$$\begin{aligned} F &= f(w_i, \alpha_1, \alpha_2, \beta_1, \beta_2, e_1^2, e_2^2, e_3^2) \\ &= w_1|S_{\mathrm{I}}| + w_2|S_{\mathrm{II}}| + w_3|S_{\mathrm{III}}| + w_4|S_{\mathrm{IV}}| + w_5|S_{\mathrm{V}}| + w_6|\mathrm{constraits}| \end{aligned} \tag{8}$$

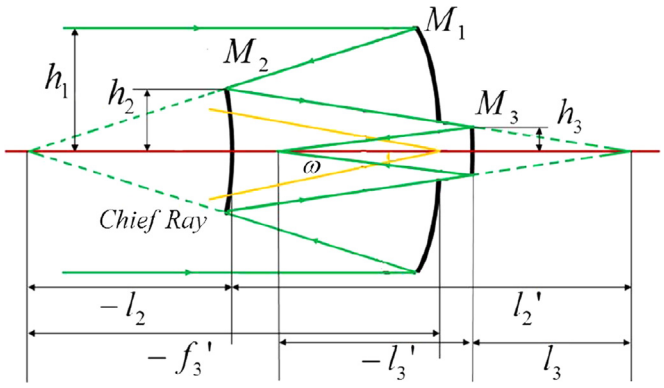

Fig. 1. The layout of the three-mirror system.

where | | is the absolute operator. w_i (i =1, 2…6) is the weight of the corresponding term, and it is set as positive. The constraints describe the requirements of the configuration. From Eq. (8), we can deduce that the value of F is positive and is influenced by the weights. An easily understood guideline can be used to determine these weights: the weights are set to higher values for the terms whose performance has a desired quality, and lower values are assigned to those that are not. Accordingly, it is the reduction of the value rather than the absolute value of F that of greater concern. The next task is to find the suitable initial structure parameters by minimizing the error function F which has 7 dimensions and is highly nonlinear. GA is adopted in this case.

2.2. Search for the reasonable initial structure via GA

The GA, which uses principles inspired by nature to "evolve" toward a best solution, is a global optimisation algorithm that does not depend on the starting parameters. GA is well-suited for high-dimensional and highly nonlinear optimisation problems [4,5,15]. Accordingly, it can be used to optimise the error function in our work. The flow chart of the design process is shown in Fig. 2

The main design process is shown in the left of Fig. 2 and is briefly described as follows:

Step 1:Aberration analysis helps to build the error function $F=f(w_i, \alpha_1, \alpha_2, \beta_1, \beta_2, e_1^2, e_2^2, e_3^2)$, as described in Section 2.1 in detail.

Step 2:Set reasonable weights and determine the structure parameters α_1, α_2, β_1, β_2, e_1^2, e_2^2 and e_3^2 by minimising the error function via GA.

Step 3:Calculate the configuration parameters R_1, R_2, R_3, d_1, d_2, and d_3 according to the Eq. (2) and Eq. (3), based on the parameters obtained in step 2.

Step 4:The usable initial structures are obtained and loaded into the optical design software for further optimization, and then, the optimised systems are obtained.

In step 2, GA is employed to determine the initial structure parameters via minimising the error function. The algorithm iteratively optimises the error function through crossover and mutation operations. The optimisation process of GA is shown in the right of Fig. 2, which is marked with a dashed pane and is

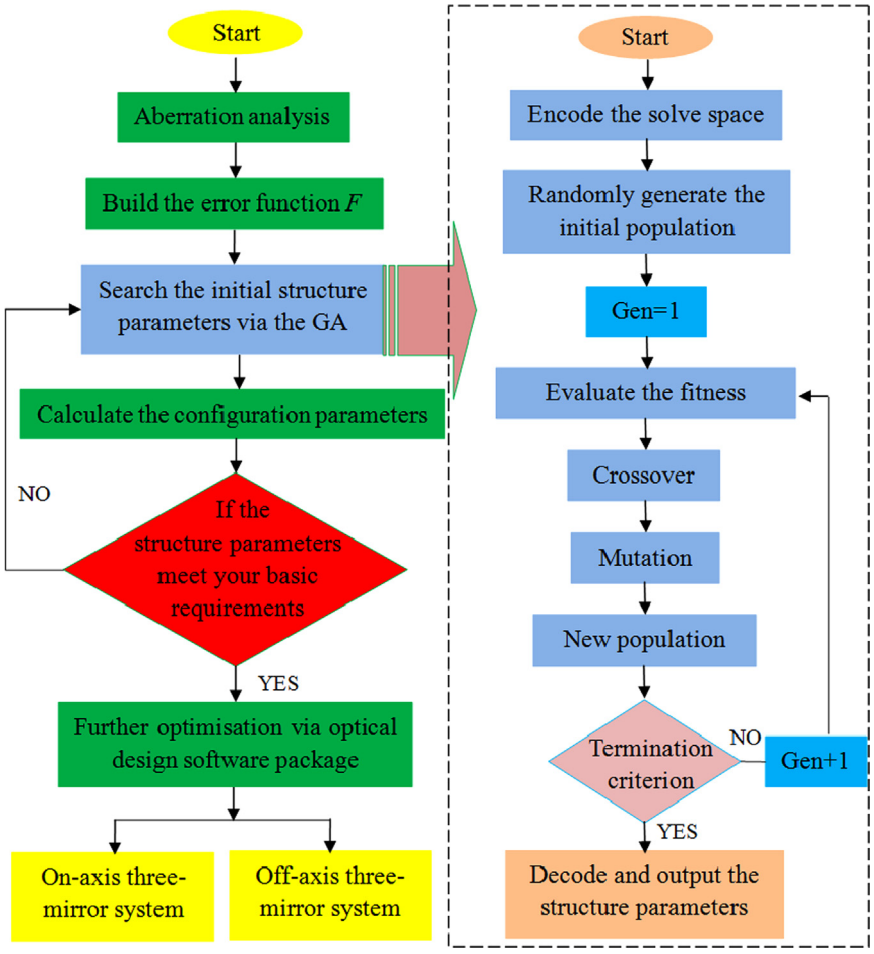

Fig. 2. Flowchart of the design process.

Table 1
The ranges of the parameters.

Parameters	α_1	α_2	$\beta_1(\times 10^3)$	$\beta_2(\times 10^{-3})$	$Conic_{M1}$	$Conic_{M2}$	$Conic_{M3}$
Ranges	[0.1,0.6]	[0.5,1]	[−1.5,−0.5]	[−1.5,−0.5]	[−5,0]	[−5,0]	[−5,0]

briefly described as follows:

Step 1:Encode the space of parameters. Here, we adopt the binary representations of genes and binary breeding template arrays filled with "1's" and "0's" representative of the chromosomes [16]. After being transformed to binary from decimal numbers, the parameters α_1, α_2, β_1, β_2, e_1^2, $e_2^2$and e_3^2 are encoded into a chromosome in order. Each chromosome denotes a possible solution of the solve space. The population is composed of those chromosomes, and the size of the population is predetermined according to the designer's experience. The evolution is based on the population.

Step 2:Evaluate the fitness. The error function F in this paper is used to evaluate each chromosome in the population. The chromosomes are ranked in ascending order of fitness. Subsequently, some pairs of chromosomes (ma and pa) are selected from the population as parents for breeding. A higher probability of selection is given to the chromosomes with a lower error function. This selection scheme can be easily implemented with a roulette wheel mechanism [15]. The number of parent chromosomes is determined by the crossover probability P_c, which is usually set from 0.9 to 1.0.

Step 3:Once the parents are selected, each parent will interchange their genes to breed a pair of children. The two-point crossover strategy is adopted in our case, in which the parents will exchange their gene segments cut by two randomly selected points to breed two children. The purpose of crossover is to breed "fitter" chromosomes by rearranging the genes.

Step 4:Mutation is a method to maintain the diversity in the population and prevent the result from being trapped in the local minimum. The children are then mutated at the point selected randomly. For mutation in binary coding, "1" will be inverted to "0" and vice versa. The mutation probability P_m is approximately 0.01.

Step 5:The next generation consists of the children and the top $(1–P_c)$ chromosomes with the lowest error function values in the current population. This procedure ensures that the elite chromosomes of each population survive to be used as the parents in the next population.

Step 6:Loop to step 2 until a termination criterion is met, usually a sufficiently low error function or a specified number of generations.

Step 7:Decode and output the structure parametersα_1, α_2, β_1, β_2, e_1^2, e_2^2 and e_3^2. Decoding is the inverse process of encoding.

3. Examples

In this section, two examples are presented to demonstrate the effectiveness of the method described in the previous section. Based on the mathematical models and principles described in Section 2, we write the appropriate programs in Matlab [17], with the parameters of the GA set according to experience: the population size is 20, $P_m=0.9$, and $P_c=0.01$. The required parameters of the optical system are as follows: objective distance $l=\infty$, and focal length $f'=1000$ mm. In this paper, all length units are millimetres.

To obtain a reasonable initial structure for a three-mirror system, the following conditions must be satisfied: $d_1<0$, $d_2>0$ and $d_3<0$. In this case, we know that $(1-\alpha_1)/(\beta_1\beta_2)>0$, $\alpha_1(1-\alpha_2)/\beta_2<0$ and $\alpha_1\alpha_2>0$. To guarantee that the rays emitted from the object reach the secondary mirror, α_1 should satisfy $\alpha_1<1$. Under the conditions described above, we set the ranges of the parameters as listed in Table 1:

3.1. On-axis three-mirror system

On-axis three-mirror systems are widely used to obtain a system with a larger aperture, with the aperture diaphragm usually located in the frame of the primary mirror. To calculate the initial structure parameters, the error function is simply composed of weighted aberrations:

$$F = \downarrow f(w_1, w_2, w_3, w_4, w_5, \alpha_1, \alpha_2, \beta_1, \beta_2, e_1^2, e_2^2, e_3^2)$$
$$\downarrow = w_1|S_{\mathrm{I}}| + w_2|S_{\mathrm{II}}| + w_3|S_{\mathrm{III}}| + w_4|S_{\mathrm{IV}}| + w_5|S_{\mathrm{V}}| \quad (9)$$

The GA is applied to search for the initial structure parameters of the on-axis three-mirror system based on the error function defined above. Five initial structures are found by changing the weights, which are presented in Table 2.

According to Eq. (2) and Eq. (3), we obtained the configuration parameters listed in Table 3.

We choose configuration 5 as our starting point because of its lower α_1, and then, we input this configuration into the design software CODE V for further optimisation; the result is an optimised on-axis three-mirror system. The configuration parameters of the optimised structure are presented in Table 4.

Comparing the configuration parameters of structure 5 between the initial and optimised cases, we find a small change in the configuration parameters. This result demonstrates that the GA works well in finding initial structures based on the error function described above.

Table 2
Parameters of the initial structures obtained using the GA for on-axis three-mirror systems.

No.	α_1	α_2	β_1	β_2	$Conic_{M1}$	$Conic_{M2}$	$Conic_{M3}$	Weights
1	0.572	0.999	−870.91	−0.0011	−0.43	−0.09	−0.50	[21111]
2	0.559	0.998	1070.48	−0.00097	−2.73	−3.62	−0.46	[12111]
3	0.595	0.999	−893.73	−0.0010	−3.76	−4.30	−0.18	[11211]
4	0.416	0.998	−1054.22	−0.00096	−0.87	−0.39	−0.04	[11121]
5	0.339	0.998	−1192.58	−0.0011	−1.38	−1.89	−0.22	[11112]

Table 3
Configuration parameters of the initial on-axis three-mirror systems.

No.	R_1(mm)	R_2(mm)	R_3(mm)	d_1(mm)	d_2(mm)	d_3(mm)
1	−1933.97	−1107.85	−1144.98	−413.69	310.88	−571.81
2	−1907.58	−1069.23	−1119.94	−419.67	583.44	−559.42
3	−2150.67	−1281.45	−1190.79	−435.32	376.45	−594.77
4	−1961.68	−818.05	−832.60	−572.20	746.12	−415.89
5	−1436.24	−488.66	−679.85	−473.99	361.97	−339.52

Table 4
Configuration parameters of the optimised on-axis three-mirror system.

Mirror	R(mm)	d(mm)	Conic
Primary	−1436.25	−473.98	−1.29
Secondary	−488.31	372.05	−1.53
Tertiary	−679.92	−339.92	−0.16

Fig. 3 a1 and b1 show the layouts of the initial structure calculated using the GA and the optimised structure obtained from the initial structure, respectively. Based on the initial structure, we attempt to extend the aperture and FOV in the further

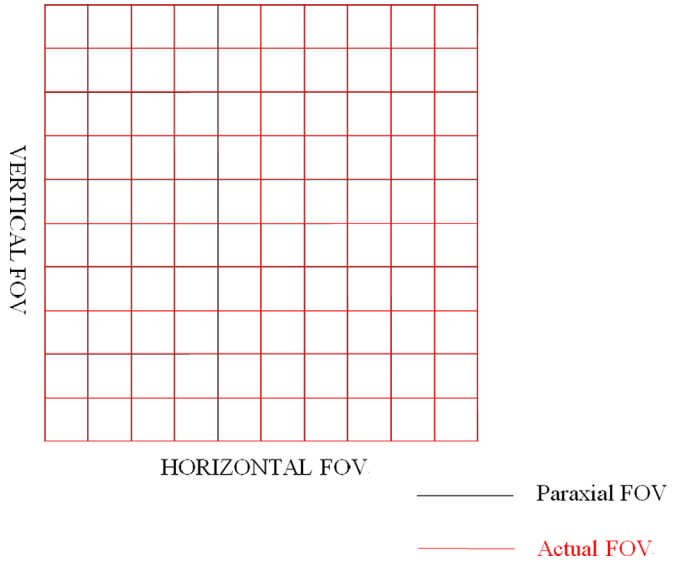

Fig. 4. Grid distortion of the optimised on-axis three-mirror system.

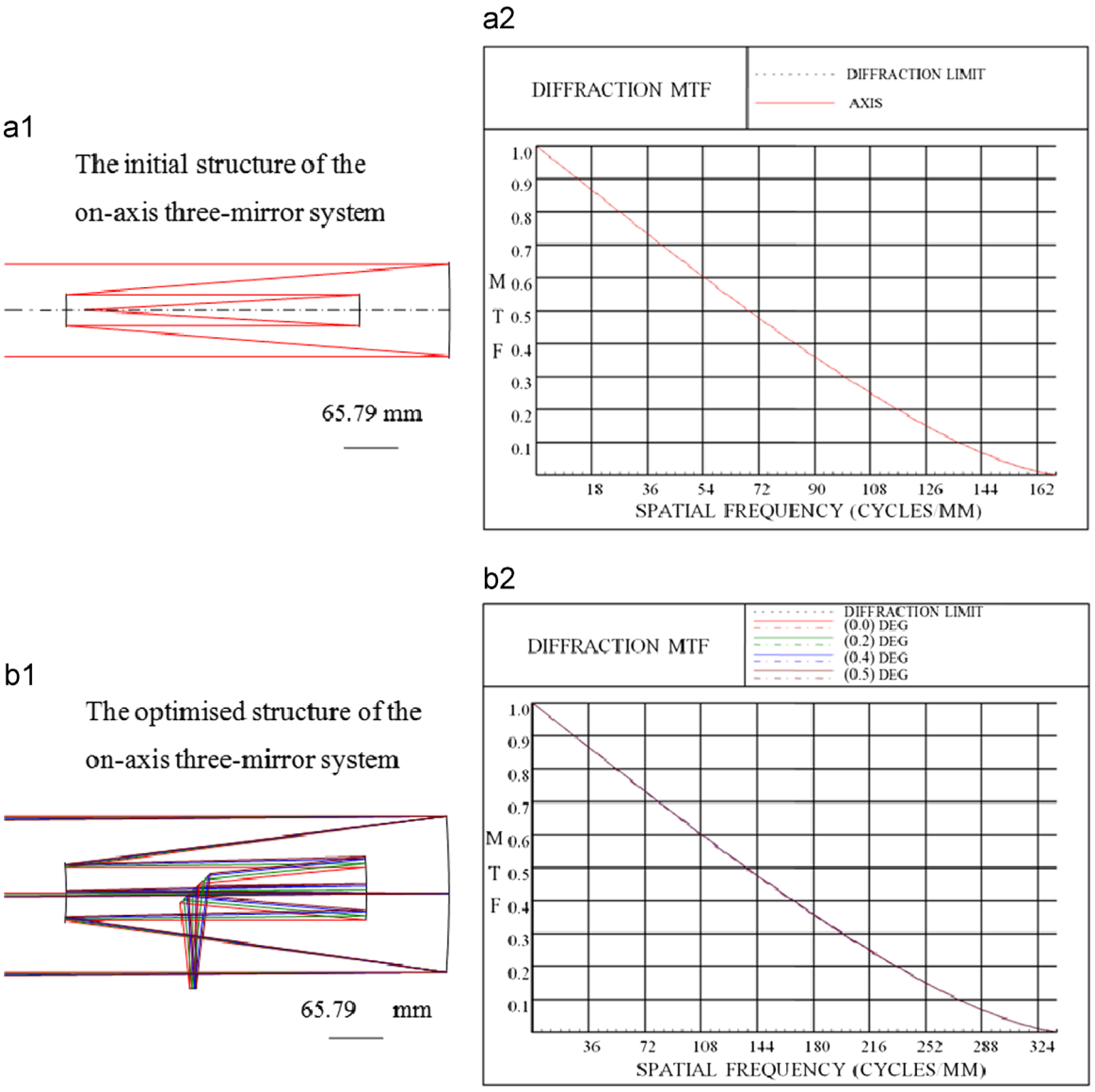

Fig. 3. Layouts (a1 & b1) and MTFs (a2 & b2) of the on-axis three-mirror system for the initial and optimised structures.

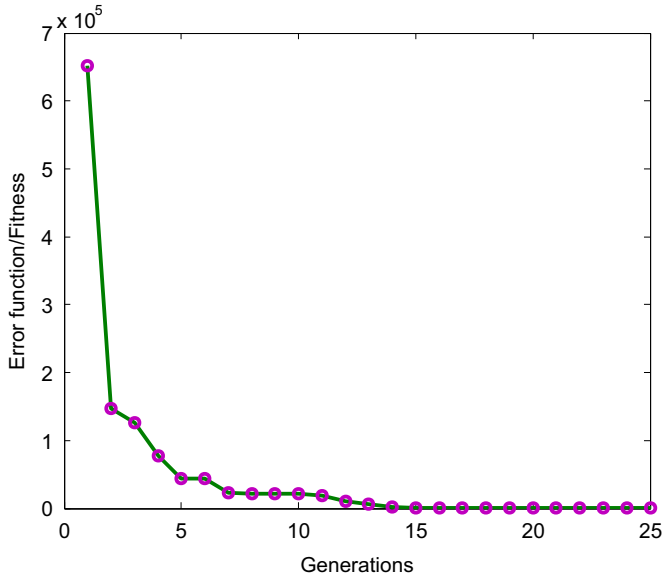

Fig. 5. Error function variation curve.

optimisation process. The FOV of the initial structure is 0 ° and is extended to 1° for the optimised structure. The systems have the same focal length of 1000 mm and different apertures: aperture of a1 is 100 mm, and the aperture of b1 is extended to 200 mm. The MTF curves for the initial and optimised structures are also presented in a2 and b2, respectively. The MTF curves show that the performance of each system is excellent almost to the diffraction limit. The optimisation result demonstrated that the initial structure has potential for further optimisation. Fig. 4 shows the grid distortion of the optimised on-axis three-mirror system. The mammal distortion is 0.02%. Fig. 5 shows the error function variation versus evolving generations. Each point at the curve is the lowest error function value in its generation. The error function decreased rapidly after 25 generations and converged to a low value close to 0. This result shows that the GA has great performance in this task.

3.2. *Off-axis telecentric three-mirror system*

Off-axis three-mirror systems are usually used to obtain a large FOV [18] and to avoid obscuring effects. To guarantee that the system is telecentric in the image space, the exit pupil of the three-mirror system should be located at infinity. Accordingly, the stop is set on the focus of the tertiary mirror. Usually, the frame of the secondary mirror is set as the stop, namely, $|d_2-1/2R_3|$ should be minimised. The error function is composed of the weighted aberrations and the constraints:

Table 6
Configuration parameters of the initial off-axis telecentric three-mirror systems.

No.	R_1(mm)	R_2(mm)	R_3(mm)	d_1(mm)	d_2(mm)	d_3(mm)
1	−2224.80	−940.90	−844.84	−642.49	421.41	−421.98
2	−1858.82	−724.26	−778.58	−567.60	388.98	−388.92
3	−1739.07	−755.30	−867.87	−492.20	433.63	−433.50
4	−1887.17	−729.64	−772.51	−579.11	387.27	−385.86
5	−1974.88	−992.25	−1003.88	−491.80	503.74	−501.54

$$f = f(w_i, \alpha_1, \alpha_2, \beta_1, \beta_2, e_1^2, e_2^2, e_3^2)$$
$$= w_1|S_I| + w_2|S_{II}| + w_3|S_{III}| + w_4|S_{IV}| + w_5|S_V| + w_6\left|d_2 - \frac{1}{2}R_3\right| \quad (10)$$

A larger value of w_6 is desired, according to the guideline described in Section 2.1, for a telecentric system. Based on the error function defined above, five results obtained via the GA are presented in Table 5.

According to Eq. (2) and Eq. (3), the configurations parameters of the five initial structures of the telecentric three-mirror system are obtained, as presented in Table 6.

The configuration parameters of initial structure 5, the fifth line of Table 6, are chosen to be loaded into the optical design software CODE V for further optimisation. To avoid the obscuring effects, we make the FOV off-axis, the FOV in the *y*-axis from 7.4° to 8.4°, and the FOV in the *x*-axis from −10° to 10°. The configuration parameters of the optimised off-axis telecentric three-mirror system are presented in Table 7. Fig. 6 shows the layouts and the performances of initial structure 5 and its optimised structure.

After further optimisation, the configuration parameters are evidently changed, while still being close to the initial structure. For the sake of minimising the aberrations over the entire FOV, fourth- and sixth-order coefficients are applied on the primary and tertiary mirrors because those additional degrees of freedom of the surfaces away from the stop are beneficial for suppressing the aberrations introduced by the wide FOV.

Theoretically speaking, when $W_6|d2-1/2R3|=0$, the chief ray will be parallel to the optical axis. Accordingly, the deviation from the chief ray to the normal line of the image plane is adopted to depict the telecentric feature. We calculate the telecentricities from 2211 (11×201) sampling of the FOV across the rectangular field area. The maximum telecentricity in sampling field points is 1.29 degrees and emerges in the edge field point.

Fig. 6 c1 and d1 shows the layouts of the telecentric initial structure calculated via the GA and the optimised structure based on the telecentric initial structure, respectively. After a simple optimisation, both the aperture and the FOV are increased. The system has a wide rectangular FOV, 1 ° in the *x*-axis and 20° in the *y*-axis. The apertures of the systems are 150 mm in size. The MTF curves for the initial structure and the optimised structure are also presented in *c*2 and *d*2, respectively. The MTFs at 50 cycles/mm are above 0.5 for all of the fields, and the results are good. Fig. 7 shows

Table 5
Parameters of the initial structures obtained via the GA for off-axis telecentric three-mirror systems.

No.	α_1	α_2	β_1	β_2	conic_{M1}	conic_{M2}	conic_{M3}	Weights
1	0.422	0.998	−860.10	−0.0010	−2.95	−4.43	−0.10	[211114]
2	0.389	0.999	−1135.66	−0.00094	−0.49	−0.36	−0.36	[121114]
3	0.433	0.999	−1154.25	−0.00099	−4.32	−6.07	−1.38	[112114]
4	0.386	0.998	−1035.97	−0.0010	−3.17	−5.15	−1.71	[111214]
5	0.501	0.999	−1019.30	−0.00099	−4.86	−7.99	−0.27	[111124]

the grid distortion of the optimised off-axis three-mirror system. The mammal distortion is 0.65%. Fig. 8 shows the error function variation versus the number of evolution generations.

4. Conclusion

A well-selected or generated initial configuration can be critical for a successful optical design, especially when the extant close configurations from which we can choose are rare. In this paper, a method for obtaining the initial structure parameters was

Table 7
Configuration parameters of the optimised off-axis telecentric three-mirror system.

Mirror	*R*(mm)	*d*(mm)	Conic	Fourth order coefficient	sixth order coefficient
Primary	−1504.31	−362.39	−6.13	−1.587e−10	1.565e−16
Secondary	−625.72	534.29	−0.89	–	–
Tertiary	−1044.35	−693.20	−1.02	−1.184e−10	−5.647e−17

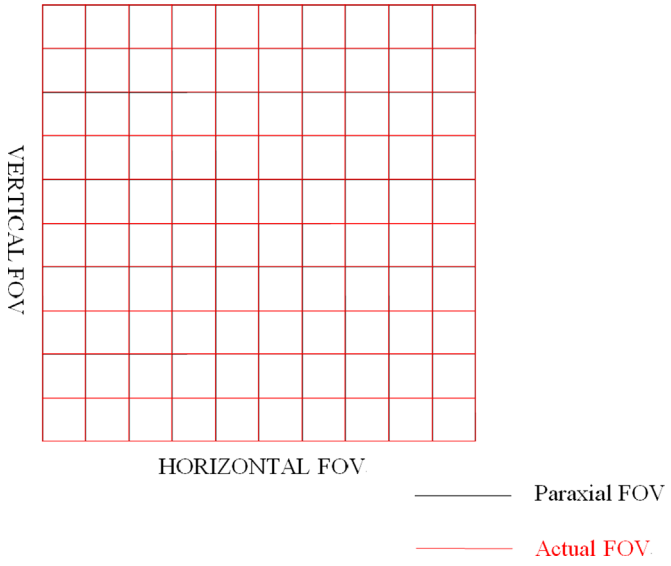

Fig. 7. Grid distortion of the optimised off-axis three-mirror system.

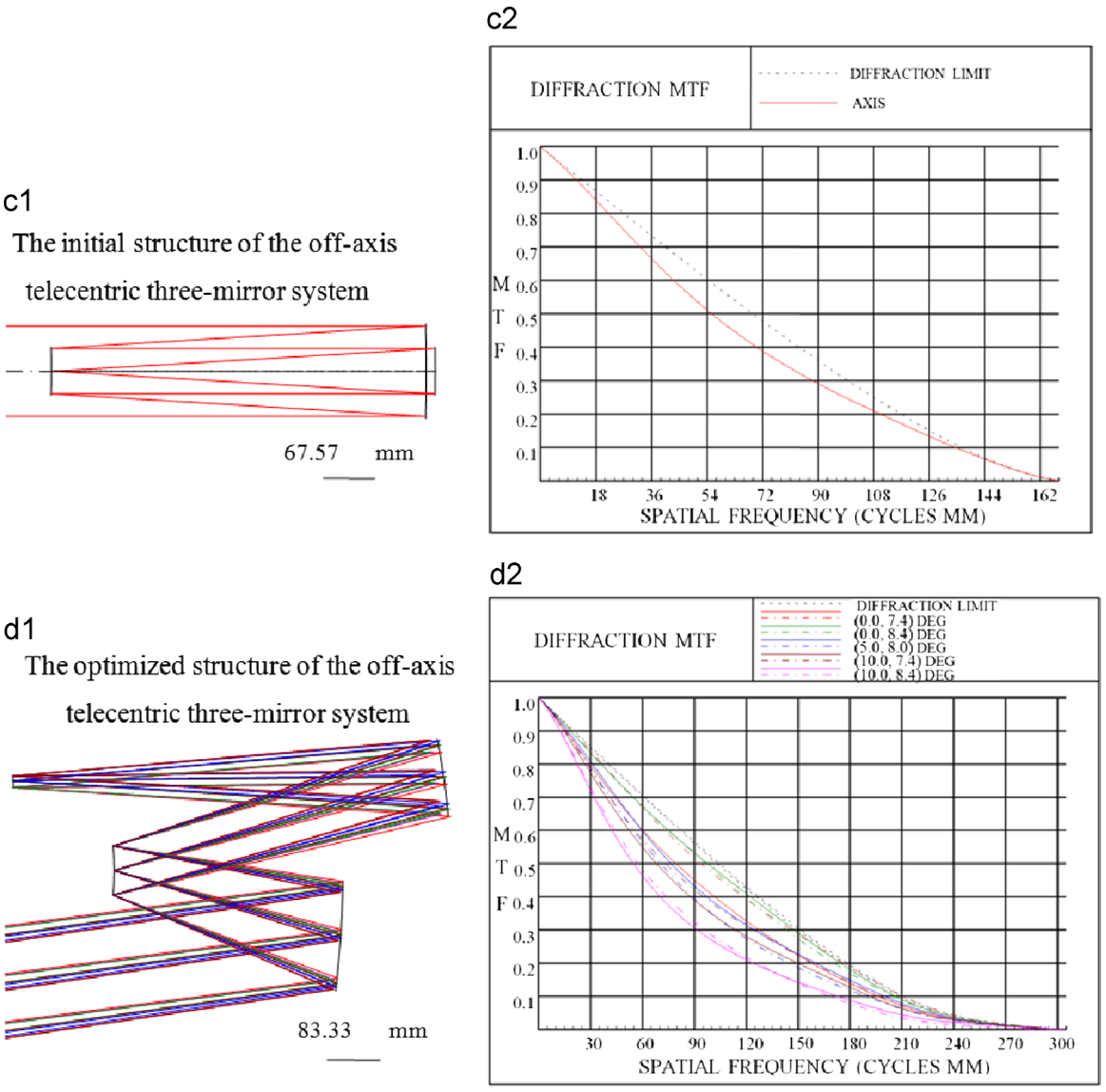

Fig. 6. Layouts (*c*1 & *d*1) and MTFs (*c*2 & *d*2) of the off-axis telecentric three-mirror system for the initial and optimised structures.

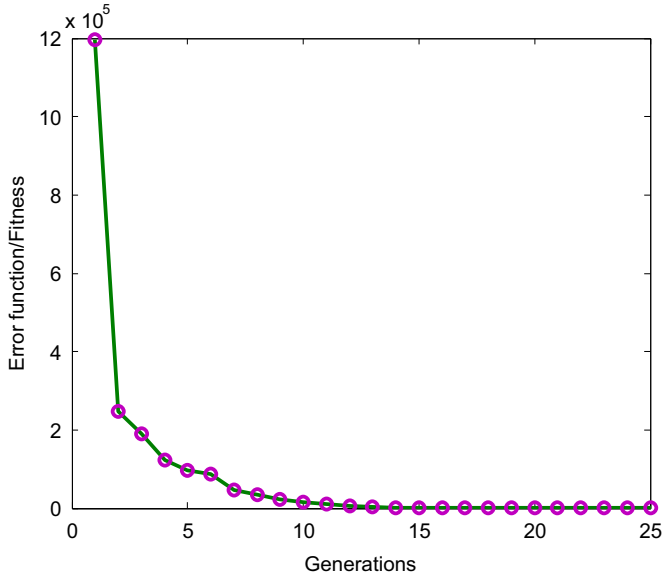

Fig. 8. Error function variation curve.

proposed. In the method, GA is employed to determine suitable initial structure parameters by minimising the error function defined by designers. The flexibility of defining the error function makes the method convenient for obtaining initial structures and meeting the design requirements. The GA's advantages in searching for the global minima in a high-dimensional and highly nonlinear parameter space make it efficient in finding suitable parameters of the initial structure. A three-mirror system is used as an example, and on-axis and off-axis telecentric three-mirror systems are obtained using proposed method. The method was demonstrated to be feasible and efficient. This method contributes to the improvement of the automatic optimisation and the reduction of the time required for determining the initial structures of optical systems. In addition to the GA, other optimisation algorithms, e.g., simulated annealing and particle swarm optimisation (PSO) and so forth, might also have the potential to solve the problem of searching for the suitable initial structure of optical system.

References

[1] Xuemin Cheng, Yongtian Wang, Qun Hao, Masakilsshiki. Global and local optimization for optical systems, Optik 117 (2006) 111–117.
[2] D. Vasiljevic, Optimization of the Cook triplet with the various evolution strategies and the damped least squares, Proc. SPIE 3780 (1999) 207–215.
[3] D. Sturlesi, D.C. O'Shea, The search for a global minimum in optical design, Proc. SPIE 1168 (1989) 92–106.
[4] R.L. Haupt, S.E. Haupt, Practical Genetic Algorithm, 2nd ed, John Wiley & Sons, United States, 2004.
[5] L. Davis, Handbook of Genetic Algorithms, Van Nostrand Reinhold, New York, 1991.
[6] Guangya Zhou, Yixin Chen, Zongguang Wang, Hongwei Song, Genetic local search algorithm for optimization design of diffractive optical elements, Appl. Opt. 38 (20) (1999) 4281–4290.
[7] Feng Yan, Xuejun Zhang, Optimization of an off-axis three-mirror anastigmatic system with wavefront coding technology based on MTF invariance, Opt. Express 17 (19) (2009) 16809–16819.
[8] Donald B. Conkey, Albert N. Brown, Antonio M. Caravaca-Aguirre, Rafael Piestun. Genetic algorithm optimization for focusing through turbid media in noisy environments, Opt. Express 20 (5) (2012) 4840–4849.
[9] D.C. van Leijenhorst, C.B. Lucasius, J.M. Thijssen, Optical design with the aid of a genetic algorithm, Biosystems 37 (3) (1996) 177–187.
[10] U. Mahlab, J. Shamir, R.H.J. Caulfield, Genetic algorithm for optical pattern recognition, Opt. Lett. 16 (9) (1991) 648–650.
[11] X. Chen, K. Yamamoto, An experiment in genetic optimization in lens design, J. Mod. Opt. 44 (9) (1997) 1693–1702.
[12] S. Ono, K. Kobeyashi, Yoshida. Global and multi-objective optimization for lens design by real-coded genetic algorithms, Proc. SPIE 3482 (1998) 110–121.
[13] ⟨http://www.opticalres.com⟩.
[14] Pan Junhua, The Design, Manufacture and Test of the Aspherical Optical Surface, Suzhou University Press, Suzhou, 2004.
[15] M.S. Zalzala, P.J. Fleming (Eds.), Genetic Algorithm in Engineering Systems, Institution of Electrical Engineers, London, 1997.
[16] N.N. Schraudolph, R.K. Belew, Dynamic parameter encoding for genetic algorithms, Mach. Learn. 9 (1992) 9–21.
[17] ⟨http://www.mathworks.com⟩.
[18] L.G. Cook, Wide field of view three-mirror anastigmatic (TMA) employing spherical secondary and tertiary mirrors, Proc. SPIE 766 (1987) 158–162.